Ferrata Storti Foundation

Targeting MCL-1 dysregulates cell metabolism and leukemia-stroma interactions and re-sensitizes acute myeloid leukemia to BCL-2 inhibition

Bing Z. Carter,[1] Po Yee Mak,[1*] Wenjing Tao,[1*] Marc Warmoes,[2] Philip L. Lorenzi,[2] Duncan Mak,[1] Vivian Ruvolo,[1] Lin Tan,[2] Justin Cidado,[3] Lisa Drew,[3] and Michael Andreeff[1]

[1]Section of Molecular Hematology & Therapy, Department of Leukemia, The University of Texas MD Anderson Cancer Center, Houston, TX; [2]Department of Bioinformatics & Computational Biology, The University of Texas MD Anderson Cancer Center, Houston, TX and [3]Bioscience Oncology R&D, AstraZeneca, Boston, MA, USA

*PYM and WT contributed equally as co-second authors.

ABSTRACT

MCL-1 and BCL-2 are both frequently overexpressed in acute myeloid leukemia (AML) and critical for the survival of AML cells and AML stem cells. MCL-1 is a key factor in venetoclax resistance. Using genetic and pharmacological approaches, we discovered that MCL-1 regulates leukemia cell bioenergetics and carbohydrate metabolisms, including the TCA cycle, glycolysis and pentose phosphate pathway and modulates cell adhesion proteins and leukemia-stromal interactions. Inhibition of MCL-1 sensitizes to BCL-2 inhibition in AML cells and AML stem/progenitor cells, including those with intrinsic and acquired resistance to venetoclax through cooperative release of pro-apoptotic BIM, BAX, and BAK from binding to anti-apoptotic BCL-2 proteins and inhibition of cell metabolism and key stromal microenvironmental mechanisms. The combined inhibition of MCL-1 by MCL-1 inhibitor AZD5991 or CDK9 inhibitor AZD4573 and BCL-2 by venetoclax greatly extended survival of mice bearing patient-derived xenografts established from an AML patient who acquired resistance to venetoclax/decitabine. These results demonstrate that co-targeting MCL-1 and BCL-2 improves the efficacy of and overcomes pre-existing and acquired resistance to BCL-2 inhibition. Activation of metabolomic pathways and leukemia-stroma interactions are newly discovered functions of MCL-1 in AML, which are independent from canonical regulation of apoptosis by MCL-1. Our data provide new mechanisms of synergy and a rationale for co-targeting MCL-1 and BCL-2 clinically in patients with AML and potentially other cancers.

Correspondence:

BING Z. CARTER
bicarter@mdanderson.org

MICHAEL ANDREEFF
mandreef@mdanderson.org

Introduction

Acute myeloid leukemia (AML) is a highly heterogeneous and aggressive hematological malignancy with dismal treatment outcomes. The survival of AML cells, including stem/progenitor cells, depends on deregulated apoptosis, which partially results from the altered expression of BCL-2 family proteins. Thus, BCL-2 family proteins are promising therapeutic targets in AML.[1,2] While combined inhibition of BCL-2 and BCL-XL caused profound thrombocytopenia,[3] a highly selective BCL-2 inhibitor, venetoclax, demonstrated potent preclinical activity, but only marginal efficacy in clinical trials in AML.[2,4] Conversely, combinations of venetoclax with hypomethylating agents have yielded complete response (CR) or CR with incomplete cell count recovery rates of >65% in elderly AML patients, but overall survival is only 10 to 17 months due to the development of resistance.[5-7]

Unlike other BCL-2 proteins, MCL-1 is short-lived and highly regulated at the transcriptional, post-transcriptional, and post-translational levels[8] in response to various stimuli. MCL-1 is required for the sustained growth of diverse oncogene-

driven hematological malignancies[9,10] and essential for AML development and AML stem cell self-renewal and survival.[11-13] MCL-1 is upregulated in about half of resistant/relapsed AML patients and associated with poor prognosis.[14] Importantly, high levels of MCL-1 expression are associated with resistance to venetoclax.[2,15,16] Furthermore, MCL-1 was reported to increase the generation of reactive oxygen species (ROS) in lung cancer cells,[17] and to positively regulate mitochondrial oxidative phosphorylation (OxPhos) in breast cancer, inducing the breast cancer stem cells, and promoting tumor chemoresistance.[18] These studies suggest that, in addition to its anti-apoptotic function, MCL-1 is coupled to tumor cell metabolism to promote cell survival. Indeed, AML cells and stem cells exhibit increased mitochondrial OxPhos,[19-21] suggesting that MCL-1 has a role in regulating mitochondrial OxPhos and altering AML cell metabolism.

Several specific MCL-1 inhibitors have been developed recently. S63845 (Servier/Novartis) was very effective and well tolerated in *in vivo* models.[22] Others such as AZD5991 (AstraZeneca)[23] and AMG176/AMG397 (Amgen)[24] have entered clinical trials. Additionally, inhibitors of CDK9 that transcriptionally regulates short-lived proteins like MCL-1 are under development as a strategy to target MCL-1, and the CDK9 inhibitor AZD4573[25] has entered clinical trials.

Rationales supporting BCL-2 and MCL-1 co-targeting have focused on apoptotic mechanisms. Targeting MCL-1 with a BIM transgene enhanced venetoclax activity against AML.[26] We reported a combinatorial regimen of BCL-2 inhibition and MDM2 inhibition-mediated p53-activation that targeted MCL-1 activity and stability. This combination was synthetically lethal to AML cells[27] and in early clinical trials elicits 40-50% CR rates among relapsed/refractory AML patients.[28] Recent studies in murine models of AML showed that the combined inhibition of BCL-2 and MCL-1 has potent antitumor activity, enhances venetoclax activity, and kills venetoclax-resistant disease.[23,24,29,30] However, the mechanisms underlying this synergism, including its effects on AML stem and venetoclax-resistant cells, have not been fully investigated.

Here, we determine the effects of MCL-1 inhibition with the novel MCL-1 inhibitor AZD5991 or the CDK9 inhibitor AZD4573 alone and in combination with venetoclax on multiple phenotypic AML stem/progenitor cell populations *in vitro* and in an *in vivo* patient-derived xenograft (PDX) model. Additionally, our *in vitro* study was conducted with bone marrow (BM)-derived mesenchymal stromal cell (MSC) co-culture, which mimics the BM stromal microenvironment.[31] In the *in vivo* study, for the first time, we utilized a PDX model derived from a patient that acquired resistance to venetoclax/decitabine treatment thus revealing a novel mechanism of synergy involving potential non-apoptotic, metabolic and microenvironmental functions of MCL-1.

Methods

Cells and treatments

AML cell lines (Molm13, MV4-11, and OCI-AML3) and primary AML cells (*Online Supplementary Table S1*) were obtained as described in the *Online Supplementary Appendix*. MCL-1-overexpressing (OE), MCL-1-knockdown (KD), and acquired venetoclax

resistant AML cells were generated as previously described.[27] BAX, BAK, or BAX/BAK double KD OCI-AML3 cells using small interfering RNA (siRNA) (control or ON-TARGETplus SMARTpool siRNA for each target, Dharmacon, Chicago, IL) were generated as previously described.[32] Human BM-derived MSC were isolated as previously described.[33] Cells, cultured under the conditions previously described[34] were treated with venetoclax, AZD5991, AZD4573, IACS-10759 (Institute for Applied Cancer Science, MD Anderson, Houston, TX), BL-8040 (BioLineRx Ltd., Israel), and various combinations without or with MSC (AML-to-MSC=4:1). For AZD4573 treatments, cells were exposed to AZD4573 for 6 hours (h), and then the drug was removed.

Cell viability assay

Viable cells and apoptosis were assessed as previously described.[34] For leukemia cells co-cultured with MSC, CD45+ cells were counted. Apoptotic cells were defined as annexin V+ and/or 7-aminoactinomycin D+ (AnnV+/7AAD+) CD45+ cells. For patient samples, annexin V positivity was determined in bulk (CD45+), CD34+CD38+/CD38-, and CD34+CD38+/CD38-CD123+ cells.

Western blot analysis and co-immunoprecipitation

Western blot analysis was conducted as described previously.[34] Antibodies used are shown in the *Online Supplementary Appendix*.

Protein determination by flow cytometry

MCL-1 and cell surface CD44 and CXCR4 were also determined by flow cytometry as shown in the *Online Supplementary Appendix*.

Adhesion and migration assay

Leukemia cells' migration and adhesion to MSC were assessed as previously described.[35]

Mitochondrial respiration assay

Mitochondrial respiration was measured using a Seahorse XF extracellular flux analyzer (Agilent Technologies, Inc., Santa Clara, CA) following the manufacturer's instructions. The oxygen consumption rate (OCR) was expressed as pmol/min/1,000 cells or relative to a control.

Reactive oxygen species and glutathione assay

Cellular and mitochondrial ROS were determined by flow cytometry after cells were stained with CellROS deep red or MitoSOX red (ThermoFisher Scientific), for 30 minutes (min) at 37°C and expressed as mean fluorescence intensity shift between stained and unstained live cells (AnnV-/DAPI-).

Total glutathione and glutathione disulfide (GSSG) were determined using a glutathione (GSH) assay kit (Cayman Chemical; Ann Arbor, MI) following the manufacturer's instructions. Reduced GSH was calculated by subtracting the amount of GSSG from total GSH.

$^{13}C_2$-1,2-glucose and $^{13}C_5$-glutamine tracing and ion chromatography-mass spectrometry metabolite analysis

Tracing and subsequence metabolite analysis are detailed in the *Online Supplementary Appendix*.

In vivo experiments

Mouse care and experiments were performed in accordance with Institution Animal Care and Use Committee approved protocols. See the *Online Supplementary Appendix* for detailed experimental procedures.

CyTOF mass cytometry

Cells were stained with metal-tagged antibodies (*Online Supplementary Table S2*) against cell surface markers, barcoded, pooled, then stained with metal-tagged antibodies against intracellular proteins and subjected to cytometry by time of flight (CyTOF) analysis as described previously.[34,36,37] Briefly, viable single cells (cisplatin-low) were gated with FlowJo (software v10.7, FlowJo LLC) and exported as flow cytometry standard (FCS) data for subsequent analysis in Cytofkit.[38] Cell populations identified and embedded by RPhenoGraph in the "Cytofkit_analyzedFCS" files were gated in FlowJo to quantify marker expression. ArcSinh-transformed counts for each protein expression in desired cell populations were visualized with heat maps.

Statistical analysis

Cell line experiments were performed in triplicates. Results were expressed as the mean ± standard error of the mean (SEM). The Student *t*-text was used to assess differences between groups; *P*-values ≤0.05 were considered statistically significant. The combination index (CI),[39] determined using Calcusyn software, was expressed as mean CI values at effective dose (ED)$_{50}$, ED$_{75}$, and ED$_{90}$. A CI<1 was considered synergistic; CI=1, additive; and CI>1, antagonistic. EC$_{50}$ and half maximal inhibitory concentration (IC$_{50}$) values were calculated using Calcusyn. Mouse survival was estimated using the Kaplan-Meier method. Survival data were analyzed using the log-rank test.

Results

MCL-1 regulates metabolic functions in acute myeloid leukemia (AML) cell lines and its inhibition decreases AML metabolism

MCL-1-KD or -OE did not alter viability of AML cell line Molm13, MV4-11, or OCI-AML3 *in vitro* (*Online Supplementary Figure S1A*). However, NSGS mice harboring MCL-1-OE Molm13 cells exhibited higher leukemia burden and succumbed sooner to AML, while mice harboring MCL-1-KD OCI-AML3 cells had decreased leukemia burden and survived longer compared with their respective controls (*Online Supplementary Figure S1B*), suggesting that MCL-1 levels affect leukemia expansion. In order to determine whether this effect requires the modulation of bioenergetic/metabolic activity, we assayed mitochondrial respiration and found that MCL-1-OE increased, whereas MCL-1-KD or inhibition with AZD5991 (at doses not affecting cell viability) decreased, OCR and ATP production in OCI-AML3 cells (Figure 1A). Compared with parental MV4-11 (MV4-11P), the venetoclax-resistant MV4-11 (MV4-11R) cells that expressed increased MCL-1[27] had higher OCR and ATP production. In both cell types, AZD5991 inhibited OCR and ATP generation (*Online Supplementary Figure S1C*). In addition, compared with controls, MCL-1-OE OCI-AML3 cells exhibited higher levels of cellular and mitochondrial ROS, lower GSH levels, and lower GSH/GSSG ratios, whereas MCL-1-KD OCI-AML3 cells displayed lower ROS, higher GSH levels, and higher GSH/GSSG ratios (Figure 1B and C).

In order to further explore metabolic functions of MCL-1, we traced ^{13}C incorporation from [13]C$_2$-1,2-glucose and [13]C$_5$-glutamine into downstream metabolites[40] using an MCL-1-KD clone (shC16) with an approximately 65% MCL-1 reduction (*Online Supplementary Figure S1D*), selected by limiting dilution of MCL-1-KD OCI-AML3 cells and OCI-AML3 cells treated with 50 nM AZD5991

(*Online Supplementary Figure S1E*). Metabolomic analysis revealed markedly lower overall incorporations of ^{13}C from both glucose and glutamine into key tricarboxylic acid (TCA) cycle intermediates including citrate, fumarate, and malate, in MCL-1-KD and AZD5991-treated OCI-AML3 cells compared to their respective controls (Figure 1D). An examination of the patterns of fractional ^{13}C enrichment from [13]C$_5$-glutamine into citrate, malate, and fumarate demonstrated increased M+4, but decreased M+3 fractional enrichment, in both AZD5991-treated and MCL-1-KD OCI-AML3 cells (Figure 1E), suggesting decreased glutamine entry into the TCA cycle accompanied by a smaller fraction of glutamine-derived carbon being used for anaplerotic reactions that fuel biosynthesis.

In both [13]C$_2$-1,2-glucose and [13]C$_5$-glutamine tracing experiments, the total amount of lactate secreted by AZD5991-treated or MCL-1-KD cells was statistically significantly lower than that secreted by their respective controls (Figure 1F). Notably, statistically significant ^{13}C enrichment (M>0) in the secreted lactate of both the AZD5991-treated and MCL-1-KD OCI-AML3 cells, was observed from [13]C$_2$-1,2-glucose, but not [13]C$_5$-glutamine (Figure 1G). Glycolysis of [13]C$_2$-1,2-glucose generates lactate with two ^{13}C labels (M+2 lactate). Thus, a reduction in M+2 lactate secretion suggests MCL-1 inhibition decreases glycolytic flux.

Next, we assessed whether the decrease in glycolytic flux was accompanied by a decrease in flux through the oxidative branch of the pentose phosphate pathway (oxPPP), a major pathway involved in the generation of the reducing equivalent NADPH that is used for ROS neutralization. When [13]C$_2$-1,2-glucose is metabolized through the oxPPP and re-enters glycolysis via the non-oxPPP, the elimination of one ^{13}C carbon through decarboxylation yields lactate containing only one [13]C. The relative oxPPP flux, which we calculated by multiplying the ratio of [M+1]/([M+1]+[M+2]) from extracellular lactate with lactate secretion rate during [13]C$_2$-1,2-glucose tracing, was lower in both AZD5991-treated and MCL-1-KD OCI-AML3 cells than in their respective controls (Figure 1H).

6-Phosphogluconic acid levels were also greatly decreased under MCL-1 inhibition (Figure 1H), in accordance with oxPPP modulation.[41] Consistent with the aforementioned extracellular flux assay results, AZD5991-treated, and MCL-1-KD OCI-AML3 cells, exhibited decreased ATP levels (Figure 1I). These findings indicated that MCL-1 inhibition downregulates key pathways that support cellular energetics in AML cells as summarized in Figure 1J. Furthermore, MCL-1 modulated the level of c-MYC in OCI-AML3 cells (*Online Supplementary Figure S1F*), which is a well-known metabolic regulator in malignant cells.

MCL-1 regulates adhesion molecule expression in acute myeloid leukemia (AML) cell lines and AML-stroma interactions

Since MSC in the BM microenvironment upregulate MCL-1, we investigated whether MCL-1 had a role in leukemia-stroma interactions. MCL-1-OE OCI-AML3 cells exhibited increased surface expression of CXCR4 and CD44, both of which participate in leukemia-MSC interactions and drug resistance, and increased OCI-AML3 migration towards, and adhesion to, MSC (Figure 2A). Conversely, MCL-1-KD OCI-AML3 exhibited decreased surface expression of CXCR4 and CD44 and decreased
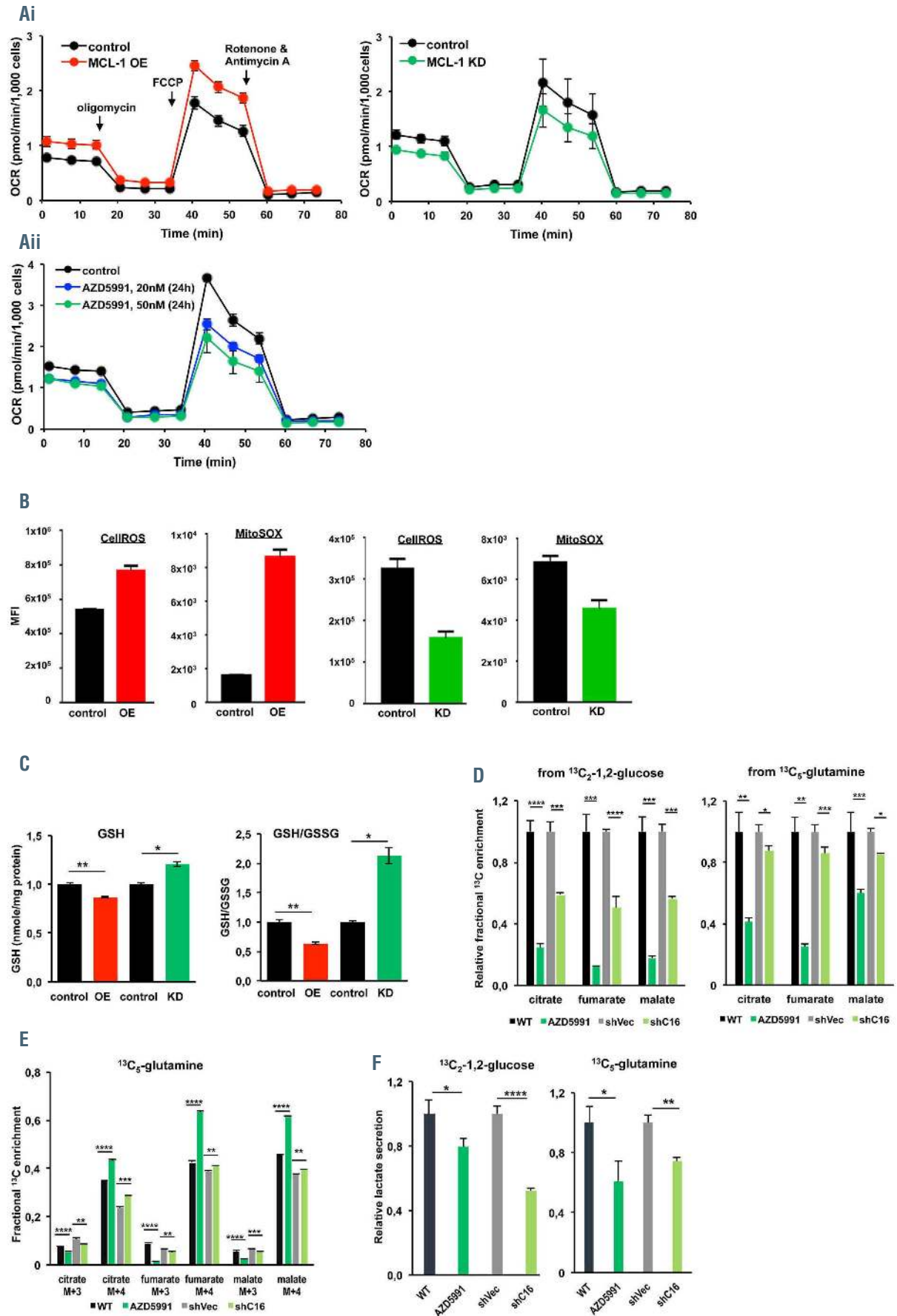
Figure 1. Continued on following page.
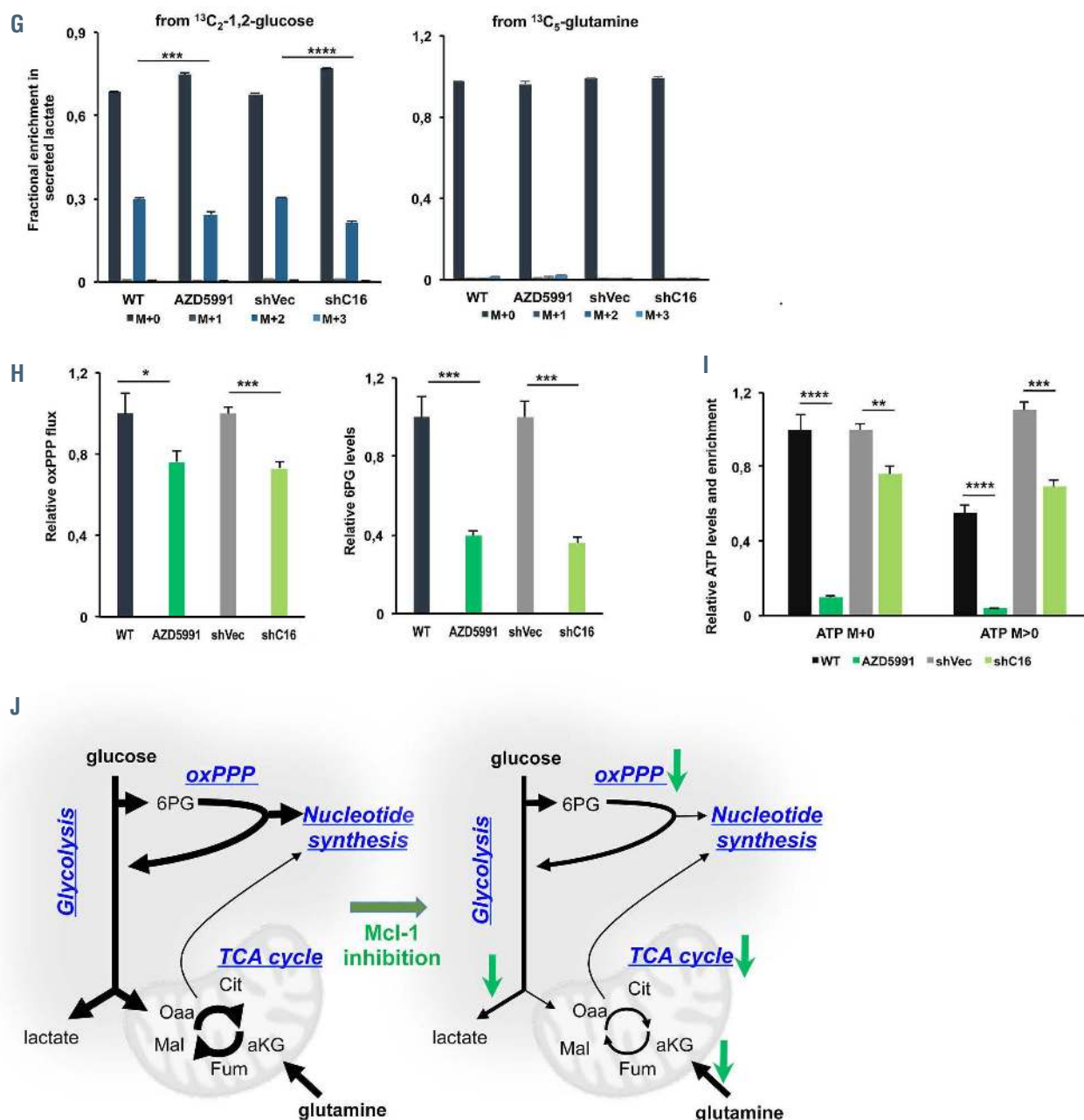
Figure 1. MCL-1 regulates cellular metabolic functions, and genetic or pharmacological inhibition of MCL-1 decreases mitochondrial respiration and metabolism in acute myeloid leukemia cells. (Ai) Seahorse analysis of mitochondrial respiration in MCL-1-overexpressing (MCL-1-OE), MCL-1 knockdown (MCL-1-KD), and (Aii) AZD5991-treated (24 h) OCI-AML3 cells. For MCL-1-OE and –KD cells, bulk populations were used unless indicated otherwise. (B) Cellular reactive oxygen species (CellROS) and mitochondrial ROS (MitoSOX) in MCL-1-OE and MCL-1-KD OCI-AML3 cells. (C) Glutathione (GSH) and GSH/glutathione and glutathione disulfide (GSSG) ratios in MCL-1-OE and MCL-1-KD OCI-AML3 cells. (D to I) OCI-AML3 MCL-1-KD clone (shC16) with an approximately 65% MCL-1 reduction (*Online Supplementary Figure S1D*) and OCI-AML3 cells treated with 50 nM AZD5991 were used for metabolomics experiments. WT: wild-type untreated control. (D) Relative enrichment of ^{13}C from ^{13}C-1,2-glucose or ^{13}C-glutamine (M>0) into key tricarboxylic acid (TCA) cycle intermediates. (E) Fractional enrichment of ^{13}C from ^{13}C-glutamine for citrate, fumarate, and malate. (F) Relative lactate levels in medium after 6 hours (h) of incubation with new medium. Lactate levels were determined by summing MS1 ion intensities for all isotopes in the ^{13}C-1,2-glucose (left) and the ^{13}C-glutamine tracer experiment (right). (G) Fractional enrichment in extracellular lactate after 6 h of incubation in the ^{13}C-1,2-glucose (left) and ^{13}C-glutamine (right) tracer experiments. (H and I) Relative pentose phosphate pathway (oxPPP) flux (left) and 6-phospho-gluconic acid (6PG) levels (right, H) and relative levels of unlabeled ATP and ^{13}C enrichment into ATP (I). Average WT and shVec M+0 levels were set to a relative level of 1. WT: parental OCI-AML3 cells; AZD5991: AZD5991-treated OCI-AML3 cells; shVec: vector control OCI-AML3 cells; shC16: MCL-1-KD OCI-AML3 cells. *$P \leq 0.05$, **$P \leq 0.01$, ***$P \leq 0.001$, ****$P \leq 0.0001$. Experiments were performed in triplicates (for seahorse analysis: duplicates for each experiment). (J) Schematic illustration of carbohydrate metabolic pathways decreased by MCL-1 inhibition. Cit: citrate; Fum: fumarate; Mal: malate; αKG: α-ketoglutarate; Oaa: oxaloacetic acid; MFI: mean fluorescence intensity.

OCI-AML3 migration toward, and adhesion to, MSC (Figure 2B). Consistently, inhibition of MCL-1 with AZD5991 decreased OCI-AML3 surface CXCR4 and CD44 expression and interaction with MSC (Figure 2C). Like other MCL-1 inhibitors, AZD5991 increased levels of MCL-1 (Figure 2C). BCL-2 inhibition with venetoclax in OCI-AML3 cells did not appreciably decrease CD44 surface expression, AML cell migration, or adhesion to MSC. However, it decreased CXCR4 surface expression (Figure 2D). These results suggest that MCL-1 enhances surface adhesion molecule expression and promotes leukemia-stroma interactions.
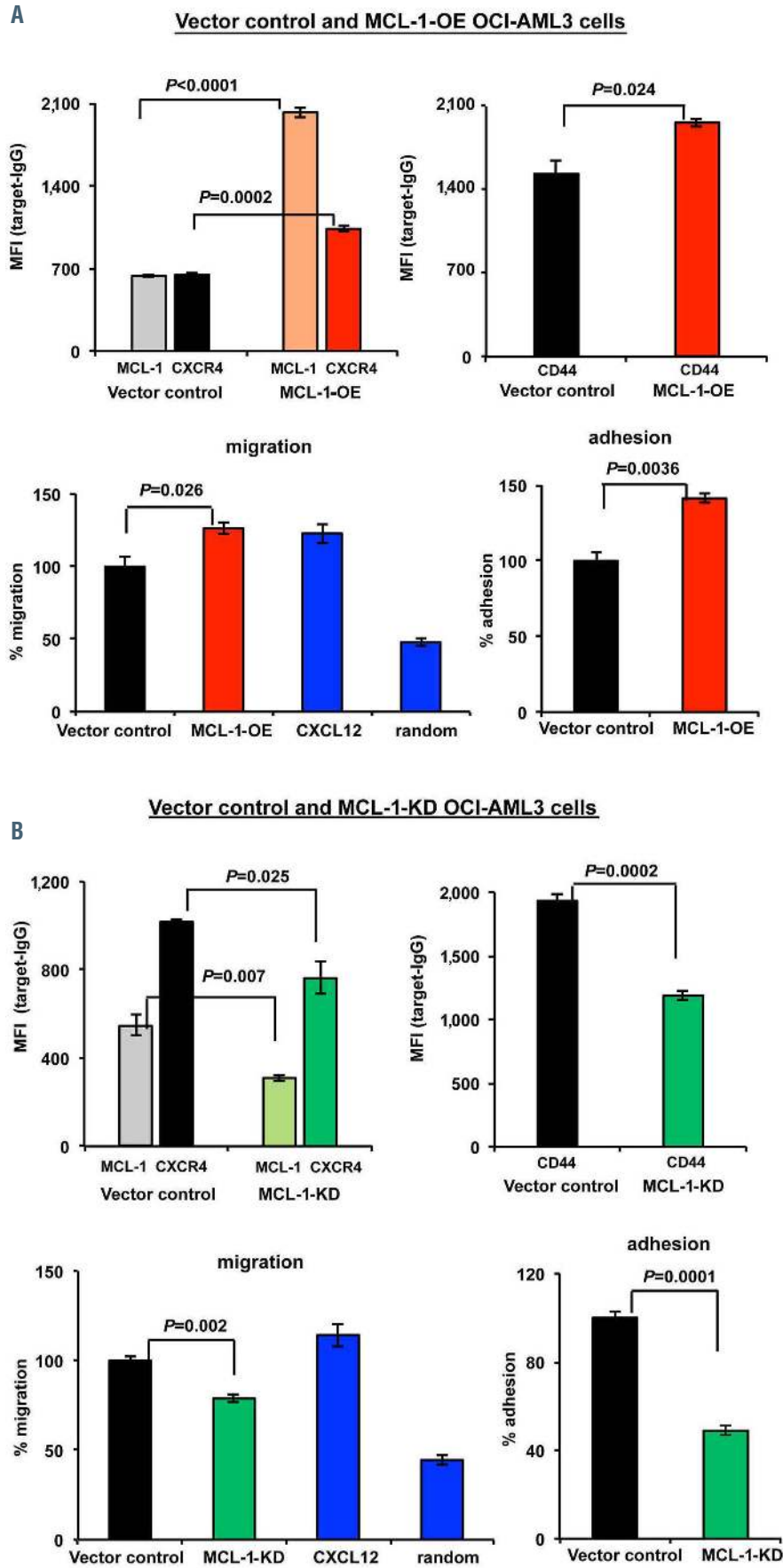
Figure 2. Continued on following page.
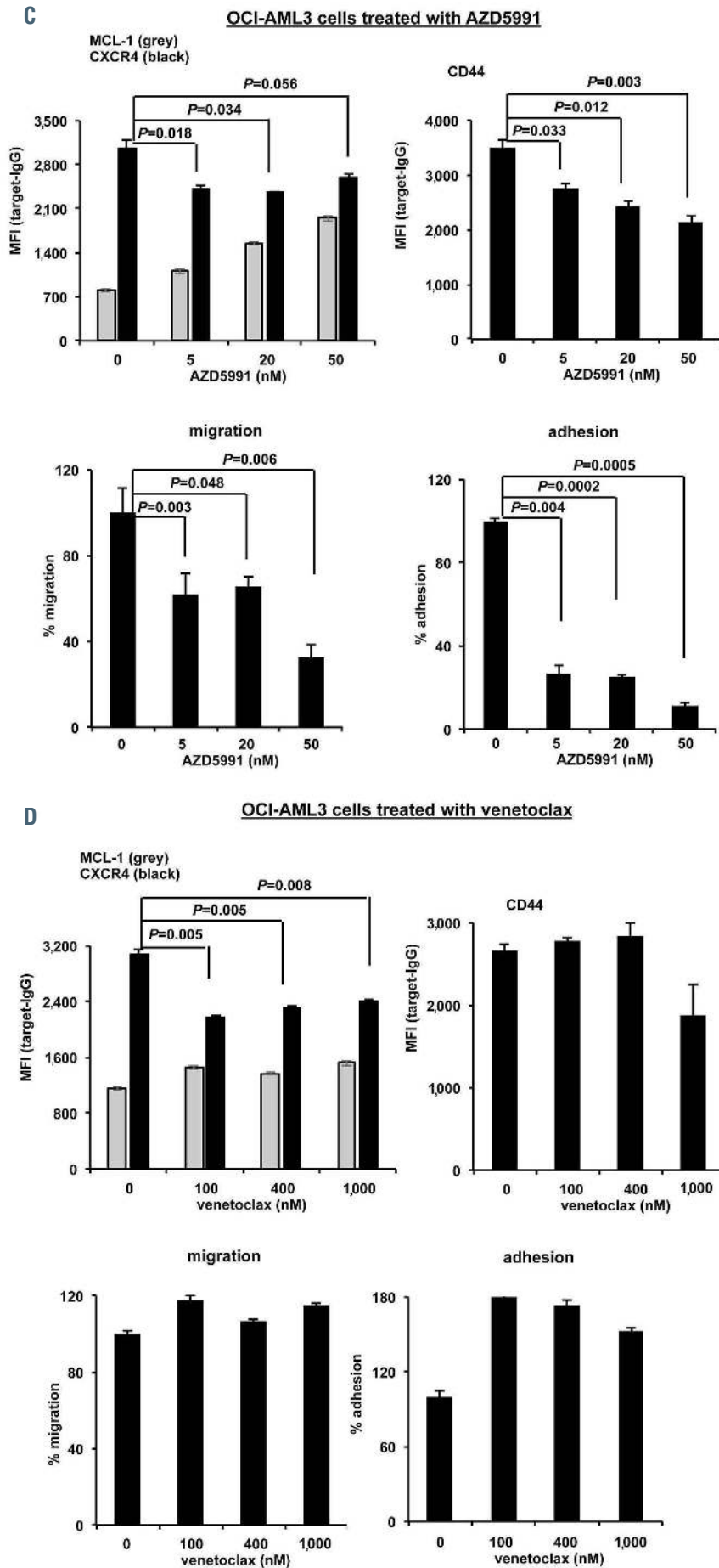
Figure 2. MCL-1 regulates cell surface expression levels of CXCR4 and CD44 in acute myeloid leukemia cells and leukemia-stroma interactions. (A and B) Cell surface CXCR4 and CD44 levels and migration and adhesion of vector control and MCL-1-overexpressing (MCL-1-OE), OCI-AML3 cells (A) or vector control and MCL-1-knockdown (MCL-1-KD) OCI-AML3 cells (B) to mesenchymal stromal cell (MSC). Blue bars represent the migration of OCI-AML3 cells to CXCL12 (positive control) or randomly (negative control). (C and D) Cell surface CXCR4 and CD44 levels and migration and adhesion of OCI-AML3 cells treated with AZD5991 (C) or venetoclax (D) for 24 hours (h) to MSC. Cell surface CXCR4 and CD44 and cellular MCL-1 levels were determined by flow cytometry. Migration was performed for 6 h and adhesion for 24 h. Experiments were performed in triplicates. Results are expressed as the mean ± standard error of the mean. IgG: immunoglobulin G; MFI: mean fluorescent intensity.

MCL-1 mediates venetoclax resistance, and its inhibition sensitizes acute myeloid leukemia cell lines to BCL-2 inhibition

Molm13 and MV4-11 cells are relatively sensitive, whereas OCI-AML3 cells are resistant, to venetoclax (*Online Supplementary Figure S2A*). Acquired venetoclax-resistant AML cell lines have increased MCL-1, but they likely also have altered levels of many other proteins. In order to determine whether MCL-1 played a key role in venetoclax resistance and whether co-targeting BCL-2 and MCL-1 overcomes this resistance, we treated MCL-

1-KD OCI-AML3 and MCL-1-OE Molm13 and MV4-11 cells with venetoclax or AZD5991. Whereas MCL-1-KD greatly sensitized OCI-AML3 cells to venetoclax (Figure 3A), MCL-1-OE Molm13 (Figure 3B) and MV4-11 cells (*Online Supplementary Figure S2B*) were largely insensitive to the drug. Responses to AZD5991 were similar, though to a lesser degree (Figure 3A and B; *Online Supplementary Figure S2B*). We then treated OCI-AML3 and MCL-1-OE Molm13 and MV4-11 cells with venetoclax plus AZD5991. The combination synergistically induced apoptosis and decreased viable cells in the intrinsically
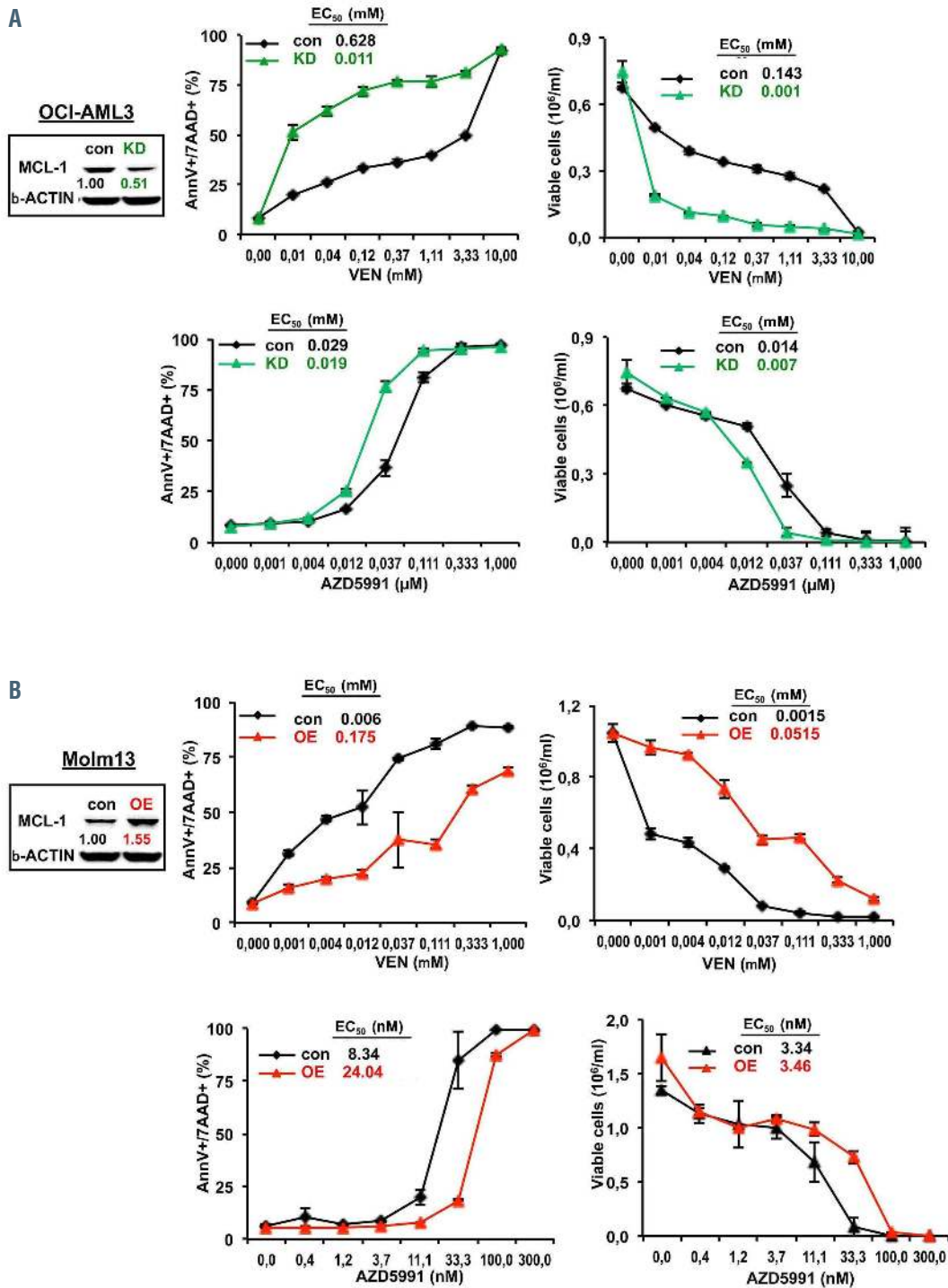
Figure 3. Continued on following page.
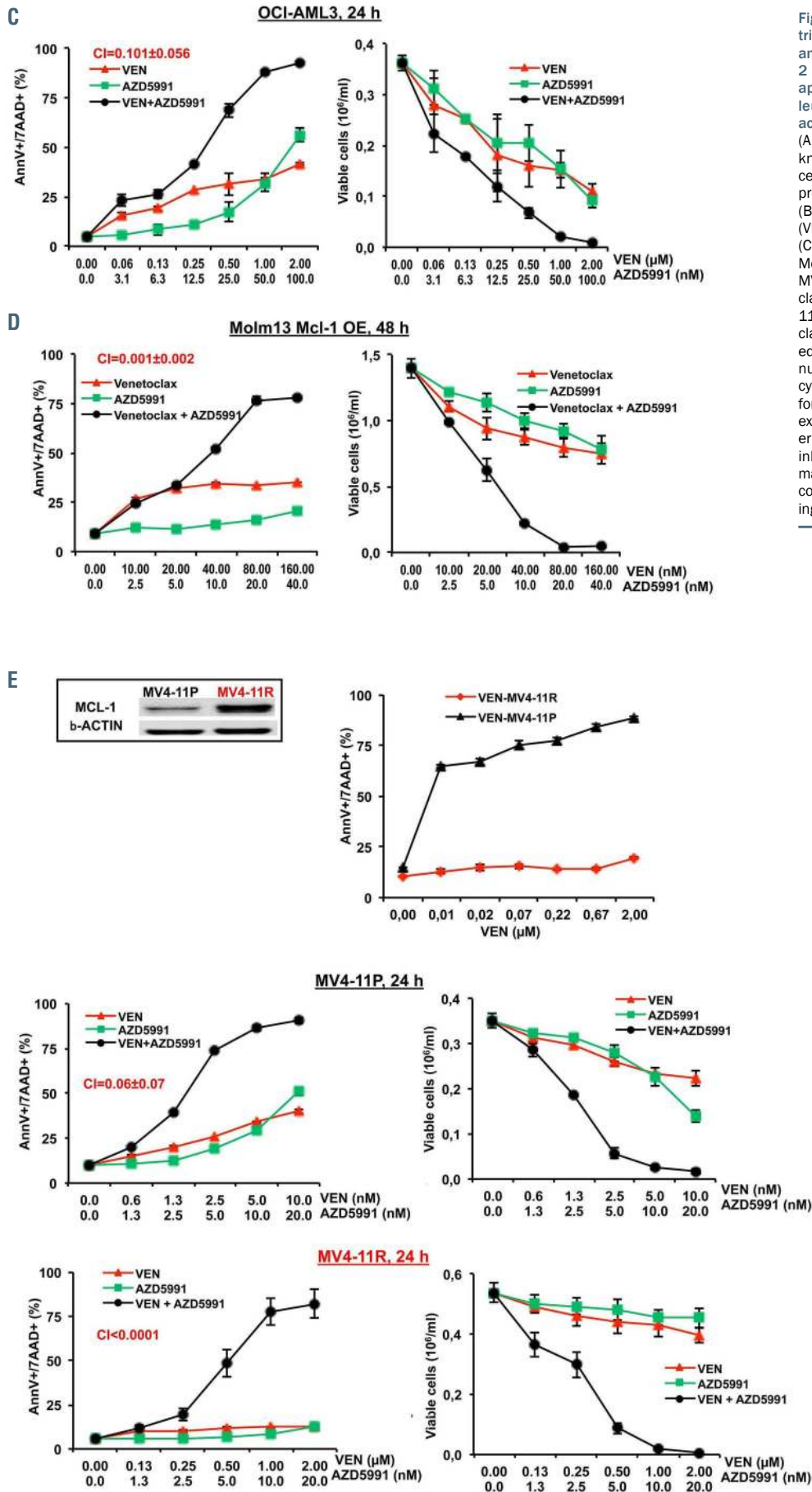
Figure 3. MCL-1 expression contributes to venetoclax resistance, and the combined inhibition of BCL-2 and MCL-1 synergistically induces apoptosis in acute myeloid leukemia cells with intrinsic or acquired resistance to venetoclax. (A and B). Control (con) and MCL-1 knockdown (MCL-1-KD) OCI-AML3 cells (A) or control and MCL-1 overexpressing (MCL-1-OE) Molm13 cells (B) were treated with venetoclax (VEN) or AZD5991 for 48 hours (h). (C to E) OCI-AML3 (C), MCL-1-OE Molm13 (D), and control parental MV4-11 cells (MV4-11P) or venetoclax-resistant MV4-11 cells (MV4-11R) (E) were treated with venetoclax and/or AZD5991 for the indicated times. Apoptosis and viable cell numbers were assessed by flow cytometry. Experiments were performed in triplicates. Results are expressed as the mean ± standard error of the mean. IC$_{50}$: half maximal inhibitory concentration; EC$_{50}$: half maximal effective concentration; CI: combination index; OE: overexpressing; KD: knockdown.

venetoclax-resistant OCI-AML3 (Figure 3C), MCL-1-OE Molm13 (Figure 3D), and MV4-11 cells (*Online Supplementary Figure S2C*). This was also the case in MV4-11R cells (Figure 3E).

We then tested CDK9 inhibitor AZD4573. AZD4573 decreased MCL-1 expression and synergized with venetoclax targeting OCI-AML3 cells (*Online Supplementary Figure S2D*). This combination was also highly synergistic against MV4-11 and MV4-11R cells (*Online Supplementary Figure S2E*). In order to demonstrate that MCL-1 is indeed the critical target regulated by CDK9, we treated MCL-1-OE Molm13 and MV4-11 cells with AZD4573 and found that, similar to the MCL-1 inhibitor AZD5991, MCL-1 OE cells were more resistant than control cells to AZD4573. Furthermore, the combination of venetoclax and AZD4573 was highly synergistic in MCL-1-OE Molm13 and MV4-11 cells (*Online Supplementary Figure S2F*).

We next treated OCI-AML3 cells with venetoclax, AZD5991, or the combination and determined interactions between anti-apoptotic BCL-2, MCL-1, and BCL-XL with the pro-apoptotic activator BIM and effectors BAX and BAK by co-immunoprecipitation to potentially understand the mechanisms of synergy. We observed that BCL-2 was bound to BIM and BAX (Figure 4A), MCL-1 was bound to BIM and BAK (Figure 4B), and BCL-XL was bound to all three (Figure 4C). Venetoclax treatment decreased BCL-2/BIM and BCL2/BAX interactions, but increased MCL-1/BIM, BCL-XL/BAX, and BCL-XL/BAK interactions. AZD5991 treatment decreased MCL-1/BIM interaction, but increased BCL-2/BIM and MCL-1/BAK interactions. When the two drugs were combined, BCL-2/BIM and BCL2/BAX interactions were largely diminished, MCL-1/BIM interaction decreased, and the single agent treatment-mediated increases of BCL-XL/BAX, BCL-XL/BAK, and MCL-1/BAK interactions were abrogated (Figure 4A to C), suggesting that the combinatorial cooperative release of activator and effector BCL-2 family proteins likely contributed to the synergy in apoptosis induction (Figure 4D).

In order to determine the contribution of metabolism and leukemia-stroma interactions on the observed synergism, we treated OCI-AML3 cells with venetoclax in the presence of the OxPhos inhibitor IACS-10759[42] or the CXCR4 inhibitor BL-8040 (4F-benzoyl-TN14003).[43] As expected, MSC co-culture protected AML cells from venetoclax-, AZD5991-, or IACS-10759-induced apoptosis (Figure 4E). While suppressing OCI-AML3 migration and adhesion to MSC, BL-8040 did not affect cell viability (Figure 4E and F). Under MSC co-culture, venetoclax activity was minimally enhanced by OxPhos or CXCR4 inhibition, but markedly augmented by combinatorial OxPhos and CXCR4 inhibition. Maximal apoptosis induction of OCI-AML3 was observed by combined MCL-1 and BCL-2 inhibition (Figure 4E). These results support that cooperative release of pro- from anti-apoptotic BCL-2 family proteins and inhibition of cell metabolism and key stromal microenvironmental mechanisms all contributed to the synergism of co-targeting MCL-1 and BCL-2 in AML cells.

Combined BCL-2 and MCL-1 inhibition synergistically induces apoptosis in primary acute myeloid leukemia (AML) cells and AML stem/progenitor cells

Primary AML cells were cultured with BM-derived MSC and treated with venetoclax, AZD5991, AZD4573, venetoclax plus AZD5991, or venetoclax plus AZD4573.

Apoptosis and viable cell counts of AML blast cells and CD34+ stem/progenitor cells were assessed and expressed as EC_{50} (Figure 5A) or IC_{50} (*Online Supplementary Figure S3*) for each agent used alone or in combination, as indicated. The patient characteristics, including mutations, venetoclax treatment status, and cytogenetics/risk categories, are shown in Figure 5B and *Online Supplementary Table S1*. Responses to venetoclax, AZD5991, or AZD4573 varied across the patient samples. Compared with the single-agent treatments, the venetoclax plus AZD5991 and venetoclax plus AZD4573 combinations were markedly more effective in inducing apoptosis and decreasing viable cell numbers (markedly lower EC_{50} and IC_{50} values, respectively) in not only blasts, but also CD34+, CD34+CD38+/CD34+CD38- and CD34+CD38+CD123+/CD34+CD38-CD123+ stem/progenitor cells in all primary AML samples, including those from venetoclax-resistant/relapsed patients (Figure 5A and B; *Online Supplementary Figure S3*; *Online Supplementary Table S1*) regardless of mutational status and cytogenetics.

Among samples 7, 8, 11, and 12 from venetoclax or venetoclax/decitabine resistant/relapsed patients, three (7, 8, and 12) had relatively high venetoclax EC_{50} values. Samples 3 and 10 that exhibited relatively high venetoclax EC_{50} values were from resistant/relapsed patients who received venetoclax after sampling and were resistant or relapsed (Figure 5A and B; *Online Supplementary Table S1*), suggesting that our *in vitro* system mirrored clinical responses. Patient samples with high venetoclax EC_{50} values tended to have high AZD5991 EC_{50} values, suggesting that AZD5991 monotherapy would be less effective in venetoclax-resistant patients. However, more samples are needed to confirm our conclusion. We observed that samples with *WT1* (3 and 12) or *BCORL1* (4 and 7) mutations were the most resistant to AZD5991 and AZD4573, respectively (Figure 5A and B). Experiments with primary AML cells treated without MSC co-culture yielded similar results (*Online Supplementary Figure S4*), but these cells were generally more sensitive to the treatments supporting the protective role of MSC. The CI values for the combinations for each AML cell population are shown in the *Online Supplementary Table S3*.

Co-targeting BCL-2 and MCL-1 exerts pronounced anti-leukemia activity in a patient-derived xenograft model of clinical venetoclax/decitabine-relapsed acute myeloid leukemia

In order to determine whether co-inhibition of BCL-2 and MCL-1 could overcome venetoclax resistance *in vivo*, we developed an AML PDX model using cells from a patient who initially responded to venetoclax/decitabine therapy, but relapsed after three cycles (Figure 6A; *Online Supplementary Table S1*). PDX-bearing mice were treated with venetoclax, AZD5991, AZD4573, venetoclax plus AZD5991, or venetoclax plus AZD4573 (Figure 6A). All treatments statistically significantly decreased circulating blasts compared to controls (*P*≤0.0001, treatment day [d] 18). The venetoclax plus AZD5991 or venetoclax plus AZD4573 group had statistically significantly fewer circulating blasts than the venetoclax (*P*<0.01) and AZD5991 (*P*<0.0001) groups or the venetoclax (*P*=0.0001) and AZD4573 (*P*<0.001) groups, respectively (Figure 6B). Analyses of BM samples (treatment d 25) yielded similar results (Figure 6C). Spleens from AZD4573- or venetoclax plus AZD4573-treated mice had a statistically significantly lower leukemia burden compared to controls, which were
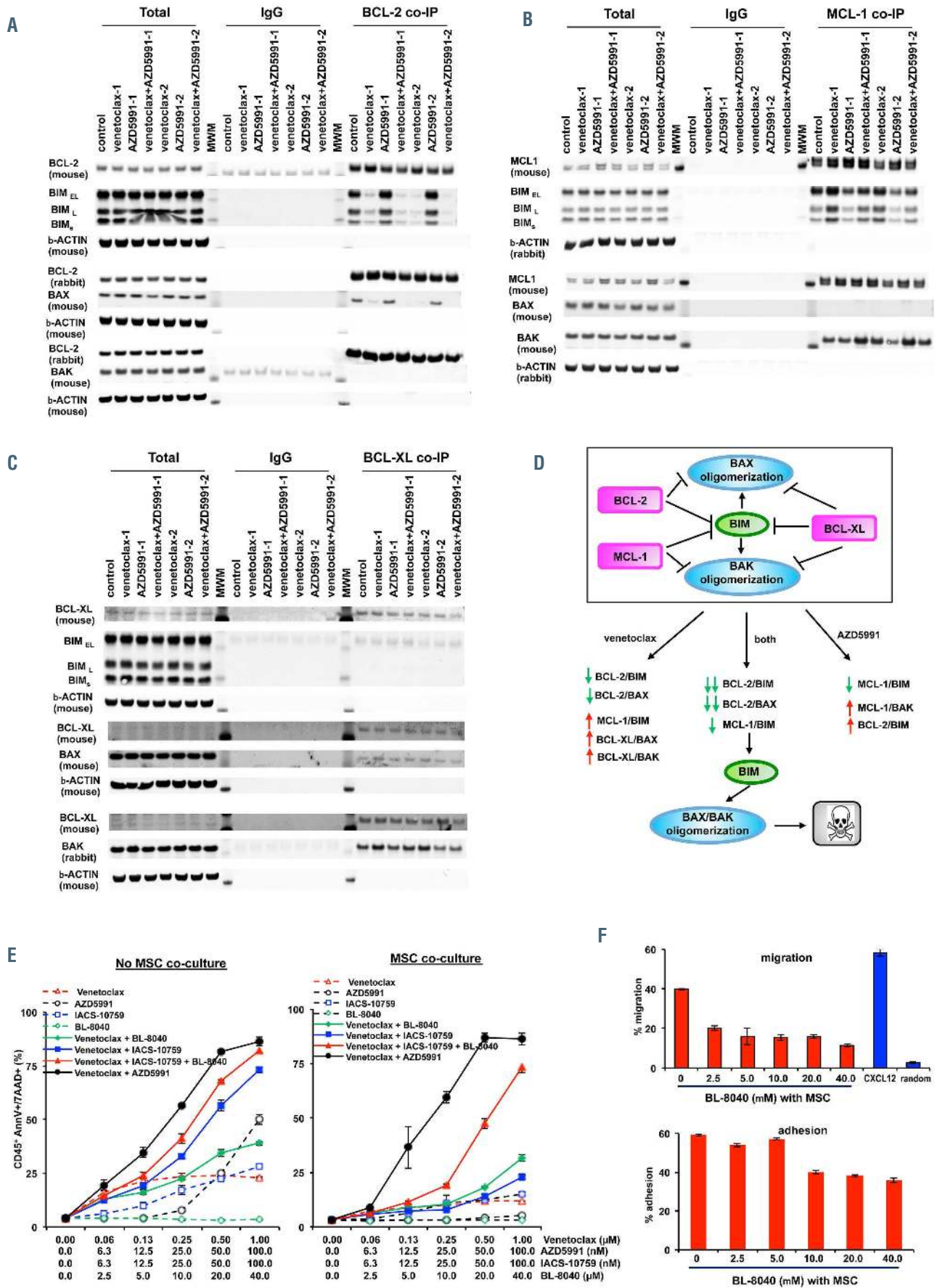
Figure 4. Legend on following page.

Figure 4. Mechanisms of synergy. Interactions of anti-apoptotic and pro-apoptotic BCL-2 proteins in control and BH3 mimetic-treated cells (A to D). OCI-AML3 cells were treated with venetoclax, AZD5991, or both (dose 1: venetoclax, 100 nM and AZD5991, 10 nM; dose 2: venetoclax, 250 nM and AZD5991, 25 nM) for 24 hours (h). (A to C) Interactions of BCL-2 (A), MCL-1 (B), or BCL-XL (C) with BIM, BAX, or BAK were determined by co-immunoprecipitation (co-IP) and western blot analysis. (D) Summary of the interactions. Roles of metabolic function and leukemia-stroma interactions (E and F). (E) OCI-AML3 cells were treated with venetoclax alone or in combination with IACS-10759, BL-8040, or AZD5991 with or without mesenchymal stromal cell (MSC) co-cultures for 48 h. Cell death in CD45$^+$ cells were determined by flow cytometry. (F) Migration (6 h) and adhesion (24 h) of BL-8040 treated-OCI-AML3 cells to MSC were measured. Migration to CXCL12 was used as a positive control and random migration as a negative control. Experiments were performed in triplicates. Results are expressed as the mean ± standard error of the mean. IgG: immunoglobulin G.

similar for spleens from the mice treated with venetoclax plus AZD5991 compared to the untreated or AZD5991-treated groups (treatment d 25, Figure 6D).

Although all the treatments statistically significantly extended survival in the PDX model, venetoclax (54 d, P=0.0035), as expected, and AZD5991 (53 d, P=0.0081) showed minimal effects similar to that presented for the *in vitro* data. AZD4573, and to greater degrees the combinations, were more effective (AZD4573: 60 d, P=0.0002; venetoclax plus AZD4573: 71 d, P=0.0005; venetoclax plus AZD5991: 76.5 d, P=0.0005 compared to controls 51 d, Figure 6E). The median survival of the venetoclax plus AZD4573 treatment group was statistically significantly longer than that of the venetoclax or AZD4573 group (P=0.0004 for both), and the venetoclax plus AZD5991 group survival was statistically significantly longer than that of venetoclax (P=0.0004) or AZD5991 group (P=0.0012) (Figure 6E). No obvious weight loss was observed during the various treatments. The mice only began to lose weight several days before they succumbed to the disease (*Online Supplementary Figure S5*). Of the 60 mice, one in AZD5991 group, one in venetoclax plus AZD5991 group, and two in venetoclax plus AZD4573 group died of treatment procedures and were not included in the survival analyses.

In order to elucidate the treatment effects on phenotypically-defined cell populations and on protein expression in these populations, we performed CyTOF analysis on BM samples (treatment d 25). Cells were clustered based on expressions of cell surface markers. While venetoclax had no, and AZD5991 and AZD4573 had minimal, effects in several AML cell populations, venetoclax plus AZD4573 and, to a greater degree, venetoclax plus AZD5991 had profound anti-leukemia activity in all cell populations including AML stem/progenitor cells (Figure 6F).

Compared to the vehicle treated controls, the single-agent treatments increased BCL-2, MCL-1, and c-MYC levels in most of the AML cell populations, whereas the combinations, particularly venetoclax plus AZD5991, decreased c-MYC in all populations, decreased BCL-2 in all but the CD34$^+$CD38$^-$ population, decreased MCL-1 in the CD45$^+$, CD34$^+$CD38$^+$CD123$^+$, and CD34$^+$CD38$^-$CD123$^+$ populations (Figure 7A). Interestingly, AZD5991, AZD4573, and, to a greater degree, venetoclax plus AZD5991 and venetoclax plus AZD4573 greatly decreased cell surface CXCR4 levels in all cell populations. AZD5991 and AZD4573 also decreased CD44 levels in all populations (Figure 7B). These results paralleled our *in vitro* findings suggesting that the inhibition of MCL-1 decreases CXCR4 and CD44 expression to suppress leukemia-stroma interactions. We also measured several signaling proteins and found that the combination treatments greatly decreased β-CATENIN and p-AKT in several AML cell populations (*Online Supplementary Figure S6A*), particularly in CD45$^+$ and CD34$^+$CD38$^-$CD123$^+$ cells (Figure 7C). Because mouse BM samples were collected 1, 3, or 2 d after venetoclax, AZD5991, or AZD4573 administration,

our analyses may underestimate the treatment effects on proteins/phosphor-proteins in leukemia cells.

We also performed CyTOF analysis on BM cells collected from moribund mice. Compared with those in controls, BCL-2, MCL-1, and c-MYC levels in all leukemia cell populations, with the exception of c-MYC in CD34$^+$CD38$^+$ cells, were higher in venetoclax, AZD5991, and the combination treatment groups (Figure 7D). Cell signaling protein analysis (*Online Supplementary Figure S6B*) showed that in all but the AZD4573 treatment CXCR4 was suppressed (Figure 7E), whereas p-AKT was greatly induced especially in the combination treatment groups (Figure 7F). Although p-AKT was not induced in the AZD4573 group, the CXCR4 level recovered compared with that observed in the controls (Figure 7E and F).

MCL-1 regulates metabolic activity in acute myeloid leukemia cells and leukemia-stromal interactions

In order to determine if MCL-1 regulates AML cell metabolic activity and leukemia-stromal interactions independent of its anti-apoptotic functions, we knocked down BAX, BAK, or both with siRNA in OCI-AML3 cells. Suppression of BAX and BAK levels were confirmed by western blot 48 h after siRNA transfection (Figure 8A). siRNA transfected cells were then treated with AZD5991 (50 nM), a dose that did not affect viable cell count (*Online Supplementary Figure S1E*). Apoptosis, mitochondrial respiration, and cell migration/adhesion to MSC were determined. As shown in Figure 8B, at the 50 nM dose of AZD5991, control siRNA-transfected cells showed no increase in apoptosis at 1 and 4 h, and only 5% more apoptotic cells over baseline at 24 h. The *Bax*, *Bak*, and *Bax* plus *Bak* siRNA-transfected cells were more resistant to AZD5991-induced apoptosis, as expected. However, inhibition of MCL-1 demonstrated the identical pattern of inhibition of mitochondrial respiration, detectable at 1 h after AZD5991 treatment, in all siRNA-transfected cells (Figure 8B). Furthermore, although AZD5991 treatment (24 h) induced low levels of apoptosis in control siRNA-transfected, but not in *Bax* and/or *Bak* siRNA-transfected OCI-AML3 cells, no apparent differences were observed in OCI-AML3 cell migration and adhesion inhibition to MSC in control, *Bax*, and/or *Bak* siRNA-transfected and AZD5991 treated cells (Figure 8C). These results suggest that MCL-1 regulates AML metabolic activity and leukemia-stromal interactions independent of its functions as an apoptosis regulator.

Finally, we treated AML patient samples (n=4) with low dose venetoclax (2.5 nM) or AZD5991 (12.5 nM) that induced low level apoptosis after 24 h (*Online Supplementary Figure S7A*) and found that AZD5991, but not venetoclax, effectively inhibited cellular and mitochondrial ROS production, reduced CXCR4 and CD44 levels, and diminished cell migration and adhesion to MSC (*Online Supplementary Figure S7B to D*), further supporting that MCL-1 regulates mitochondrial respiration and leukemia-stromal-interactions in AML.

A

B

Figure 5. Combined inhibition of BCL-2 and MCL-1 synergistically induces apoptosis in primary acute myeloid leukemia (AML) cells and AML stem/progenitor cells under mesenchymal stromal cell co-culture conditions. Primary acute myeloid leukemia (AML) cells co-cultured with mesenchymal stromal cellc (MSC) were treated with venetoclax (VEN), AZD5991, AZD4573, VEN plus AZD5991, or VEN plus AZD4573 for 48 hours (h). The apoptosis of blast cells and stem/progenitor cells were assessed by flow cytometry. (A) Half maximal effective concentration (EC$_{50}$) values of venetoclax alone or combined with AZD5991 or AZD4573, of AZD5991 alone or combined with venetoclax and of AZD4573 alone or combined with venetoclax in blast cells and stem/progenitor cells from individual patient samples are shown. Samples lacking the indicated cell populations or that had excessively high spontaneous apoptosis are not represented. *>3,000 nM. (B) Mutations, venetoclax treatment status, and cytogenetics/risk category of each patient from whom primary AML samples were obtained. HR: complex cytogenetics and high risk; IR: intermediated risk.

Discussion

Here, we demonstrate that co-targeting BCL-2 and MCL-1 is highly effective in AML cell lines and primary patient samples, which is consistent with recent reports.[23,24,26,29] Importantly, combined MCL-1 and BCL-2 inhibition was highly synergistic against AML stem/progenitor cells and exerted pronounced anti-leukemia activity in venetoclax-resistant AML patient samples *in vitro*, even under conditions mimicking the BM stromal microenvironment. Furthermore, similar findings were obtained in a unique PDX model of clinical venetoclax/decitabine-relapsed AML. Hence, the combination is not just more effective than each agent given alone, but has the potential to overcome intrinsic and acquired venetoclax resistance. In exploring the mechanisms underlying the combination's efficacy, we demonstrated that targeting MCL-1 sensitizes to BCL-2 inhibition in AML through not only cooperative release of pro-apoptotic from binding to anti-apoptotic BCL-2 proteins but also inhibition of cell metabolism and key stromal microenvironmental mechanisms. The metabolic and stromal functions of MCL-1 can apparently act independently of the protein's anti-apoptotic activity. These findings provide rationale for the clinical development of combined BCL-2 and MCL-1 targeting in resistant/relapsed AML patients, particularly in patients who were resistant/relapsed from venetoclax-based therapies.

We observed that *WT1*- or *BCORL1*-mutated primary AML samples were particularly resistant to AZD5991 and AZD4573, respectively. *WT1* mutation in AML is associated with poor outcomes and chemoresistance,[44] and *BCORL1* encodes a transcription co-repressor, opposite to CDK9. We speculate that *BCORL1*-mutated cells are less transcriptionally suppressed, and therefore more resistant to CDK9 inhibition. However, the sample size for either
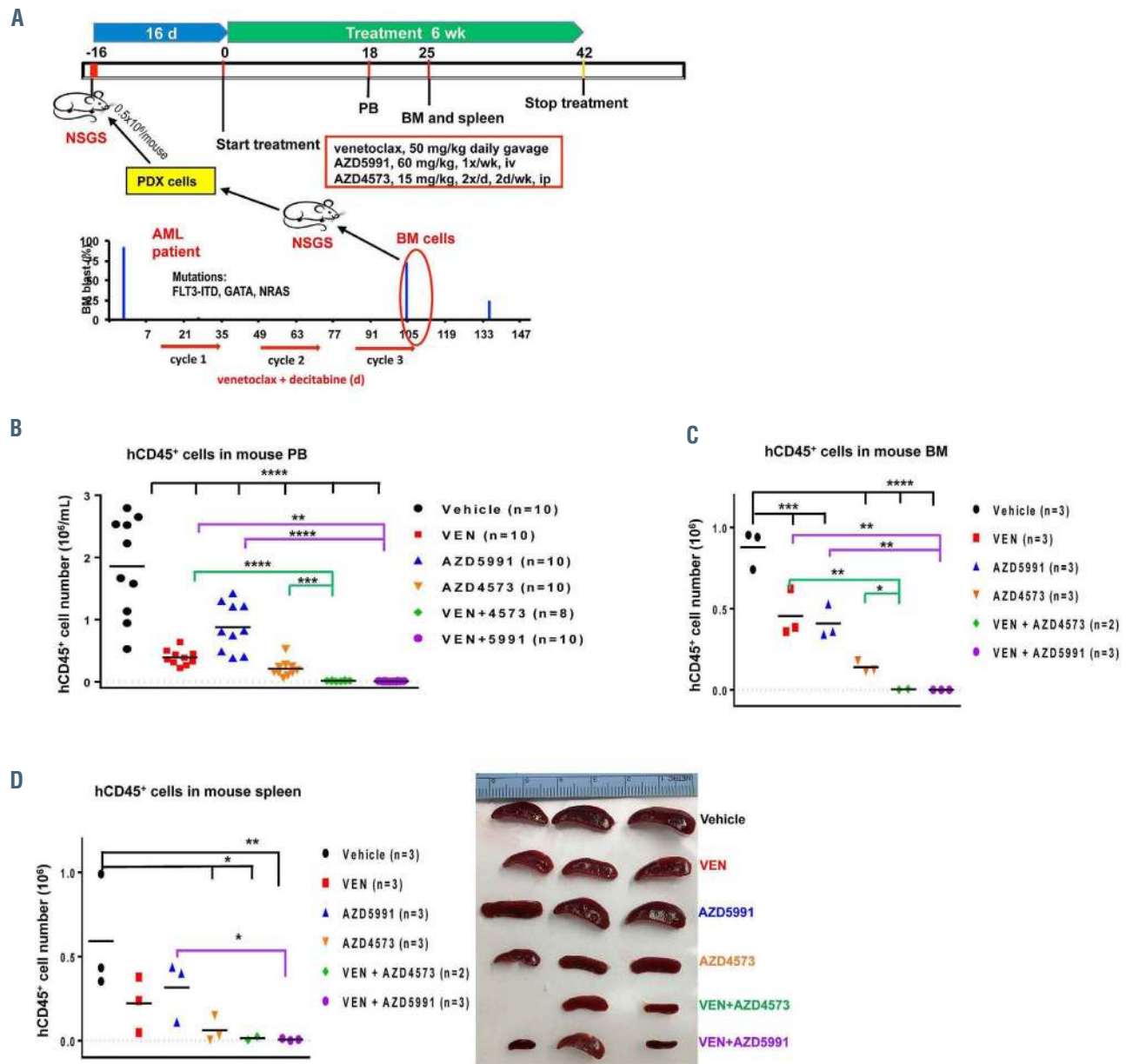
Figure 6. Continued on following page.

E

F
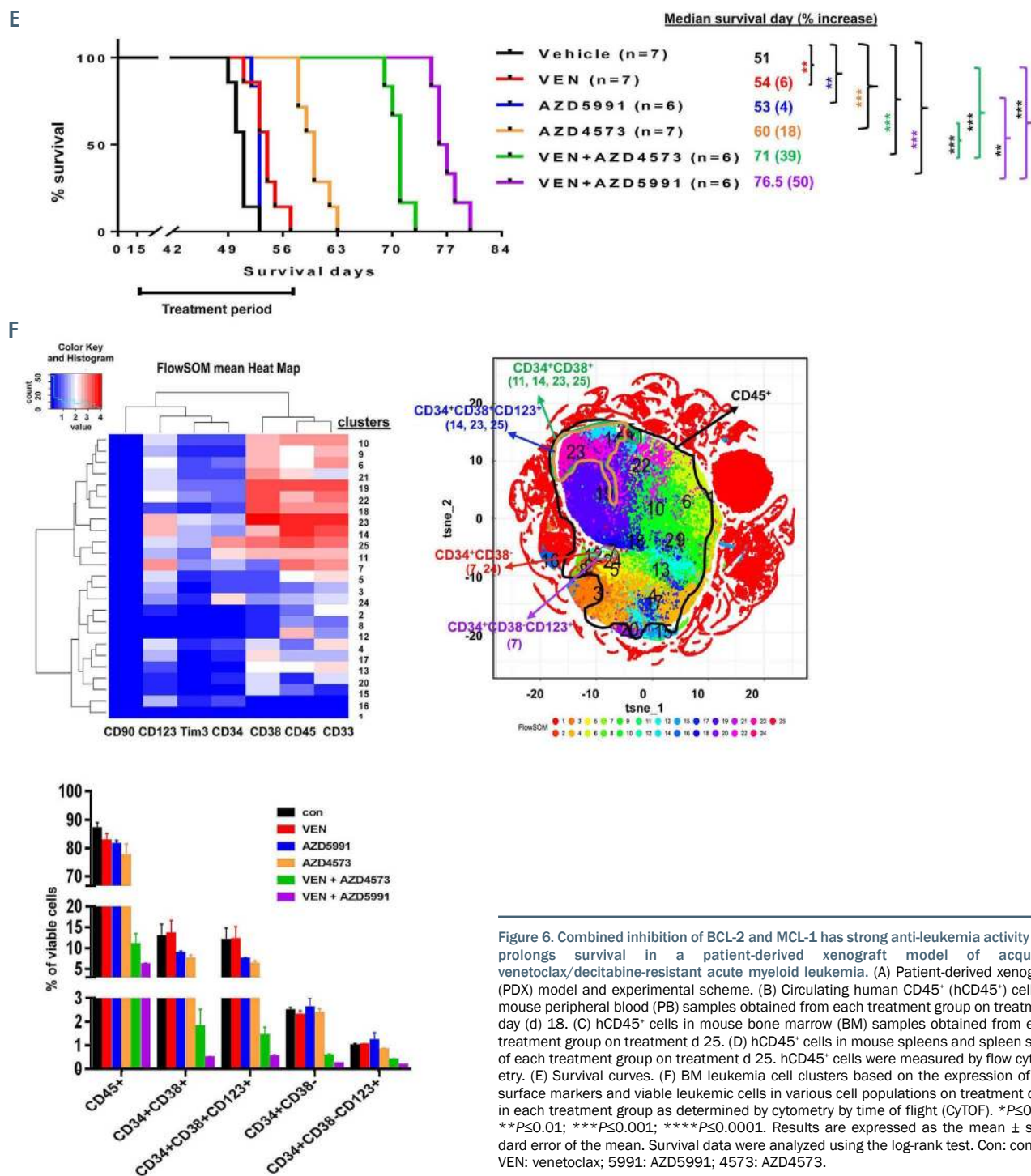
Figure 6. Combined inhibition of BCL-2 and MCL-1 has strong anti-leukemia activity and prolongs survival in a patient-derived xenograft model of acquired venetoclax/decitabine-resistant acute myeloid leukemia. (A) Patient-derived xenograft (PDX) model and experimental scheme. (B) Circulating human CD45^{+} (hCD45^{+}) cells in mouse peripheral blood (PB) samples obtained from each treatment group on treatment day (d) 18. (C) hCD45^{+} cells in mouse bone marrow (BM) samples obtained from each treatment group on treatment d 25. (D) hCD45^{+} cells in mouse spleens and spleen sizes of each treatment group on treatment d 25. hCD45^{+} cells were measured by flow cytometry. (E) Survival curves. (F) BM leukemia cell clusters based on the expression of cell surface markers and viable leukemic cells in various cell populations on treatment d 25 in each treatment group as determined by cytometry by time of flight (CyTOF). *$P \leq 0.05$; **$P \leq 0.01$; ***$P \leq 0.001$; ****$P \leq 0.0001$. Results are expressed as the mean ± standard error of the mean. Survival data were analyzed using the log-rank test. Con: control; VEN: venetoclax; 5991: AZD5991; 4573: AZD4573.

WT1- or *BCORL1*-mutated cells was too small to draw definitive conclusions. Additional studies are needed to confirm our finding, which may help guide patient selection.

In contrast to a recent study showing that venetoclax-resistant cells are more sensitive to the MCL-1 inhibitor VU0661013,[30] we found that intrinsic or acquired venetoclax resistant AML cells were less responsive to the MCL-1 inhibitor AZD5991, but the combination of venetoclax and AZD5991 or AZD4573 synergistically induced cell death regardless of the single-agent response, both *in vitro* and *in vivo*. These data suggest that patients whose disease is resistant to, or relapses from, venetoclax therapy may

potentially benefit from co-targeting MCL-1 and BCL-2.

In order to understand the mechanisms of synergy, especially in cells insensitive to BCL-2 or MCL-1 inhibition alone, we examined the interactions of anti- and pro-apoptotic BCL-2 proteins in OCI-AML3 cells treated with venetoclax, AZD5991, or both. Targeting either BCL-2 or MCL-1 decreased the interactions of one of them with pro-apoptotic BCL-2 proteins, but increased the interactions of the other with pro-apoptotic proteins. Only when both are inhibited, maximal amounts of unbound activator protein BIM and effector proteins BAX/BAK become available, and more effectively induce apoptosis.

Interestingly, Pollyea *et al.* recently attributed the effec-
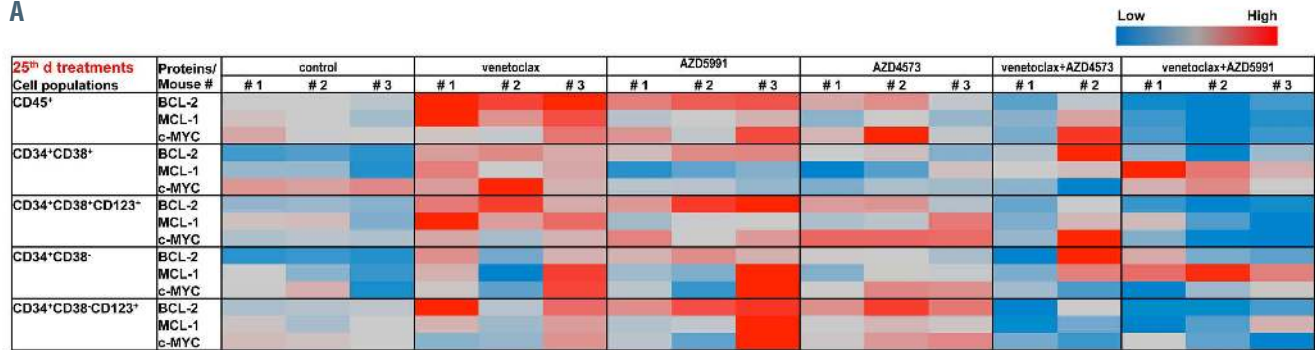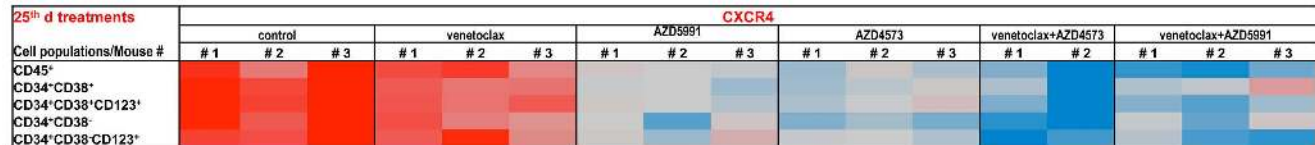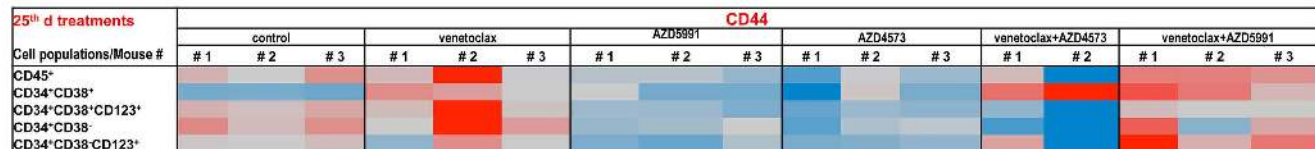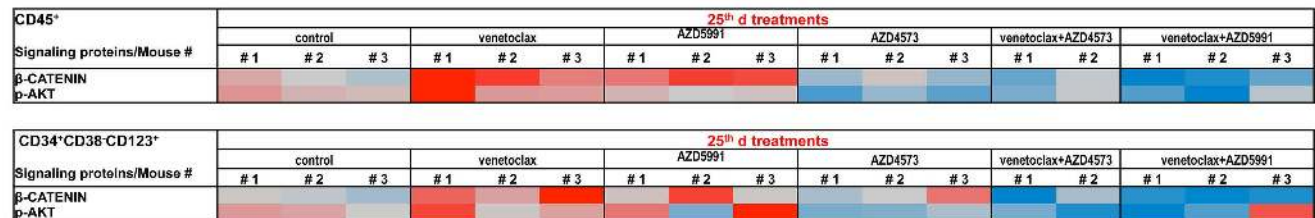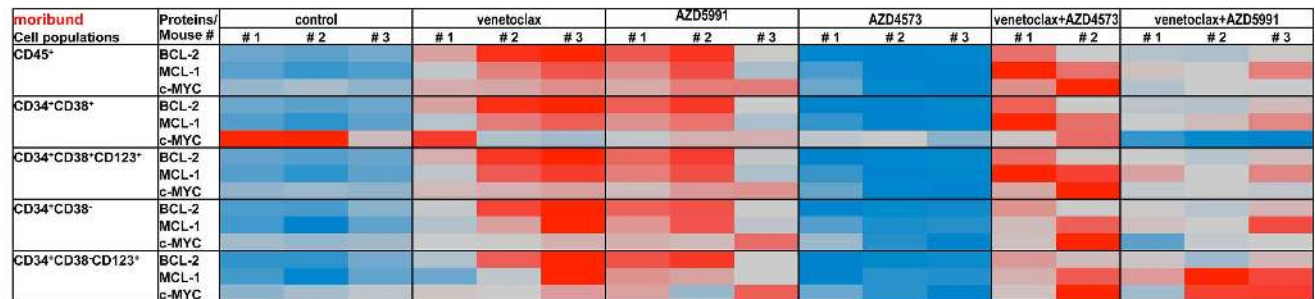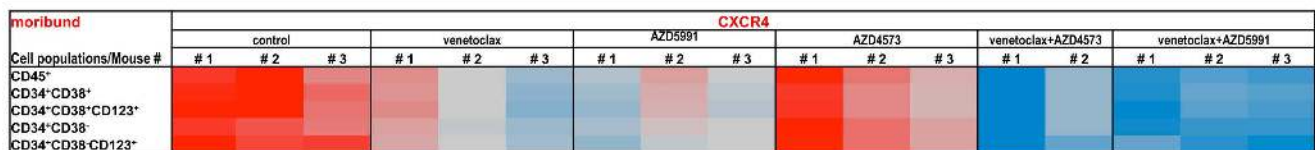
Figure 7. Legend on following page.

Figure 7. Protein levels in various leukemia cell populations in mouse bone marrow as determined by CyTOF. Bone marrow (BM) cells were collected from the mice on day (d) 25 of treatment (A to C) or from moribund mice (D to F) from each treatment group (n=2 or 3 mice/group). (A and D). BCL-2, MCL-1, and c-MYC levels in various leukemia cell populations in each treatment group. (B and E) Cell surface expression levels of CXCR4 and CD44 (B) or CXCR4 (E) in various cell populations in each treatment group. (C) β-CATENIN and p-AKT levels in CD45+ and CD34+CD38·CD123+ cells. (F) p-AKT levels in various cell populations. The protein levels of individual samples are presented as heat maps. After stained with antibodies against cell surface markers, all BM samples collected at d 25 treatment were barcoded, pooled into the same tube, stained, and run concomitantly and all BM samples collected from moribund mice were barcoded, pooled into the same tube, stained, and run concomitantly.

tiveness of the venetoclax plus azacitidine combination in its ability to suppress OxPhos, disrupt the TCA cycle, and perturb cell energy metabolism, thereby efficiently targeting leukemia stem cells, an effect that was not achieved with the venetoclax treatment alone.[7] We found that MCL-1 regulates redox and metabolic functions in AML cells and that genetic or pharmacological inhibition of MCL-1 suppressed several cellular energetic and metabolic

pathways, including TCA cycle, glycolysis, and PPP. We further demonstrated that inhibiting this function of MCL-1 contributed to the enhanced activity of venetoclax against AML cells.

ROS stabilize HIF1 thereby activating hypoxia signaling.[45,46] Although MCL-1 alteration in AML cells did not elicit detectable changes in HIF1α levels, it elicited changes in CXCR4, a HIF1α target, and CD44. Both, the
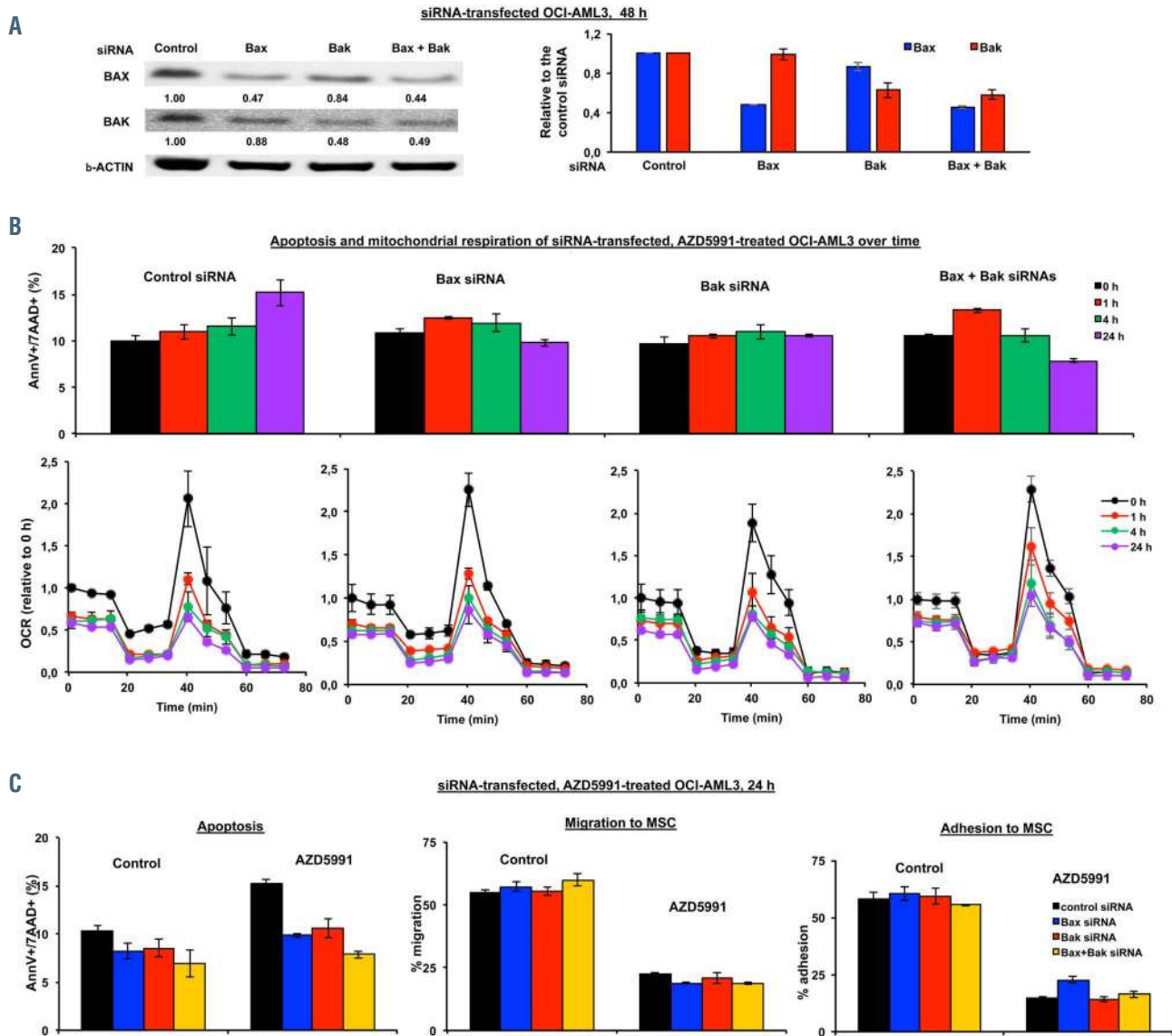
Figure 8. Effects of BAX and/or BAK knockdown on apoptosis, mitochondrial respiration, and migration/adhesion to mesenchymal stromal cell of acute myeloid leukemia cells in responses to MCL-1 inhibition. OCI-AML3 cells were transfected by electroporation with control, Bax, Bak, or Bax and Bak small interfering RNA (siRNA) (4 μM) for 48 hours (h) and then treated with AZD5991 (50 nM) for 24 h. (A) BAX and BAK levels in siRNA-transfected OCI-AML3 cells at 48 h, determined by western blot. The left panel is the result of a representative experiment and the right is the quantitative results of three independent experiments. (B) Apoptosis by flow cytometry and mitochondrial respiration by Seahorse of siRNA-transfected OCI-AML3 cells treated with AZD5991 at various time points. (C) Apoptosis and migration (6 h) and adhesion (24 h) of siRNA-transfected OCI-AML3 cells treated with AZD5991 for 24 h compared with untreated controls. The experiments were performed in triplicates (with duplicates for each experiment in the Seahorse experiment). The results are expressed as mean ± standard error of the mean. AnnV: annexin V; OCR: oxygen consumption rate. MSC: mesenchymal stromal cells.

CXCR4/CXCL12 axis and CD44 are critical for leukemia-BM stromal microenvironment interactions. Indeed, we found that genetic or pharmacological manipulation of MCL-1, but not BCL-2, in AML cells altered cell migration and adhesion to MSC. In confirmation, *in vivo* MCL-1, but not BCL-2, inhibition decreased CXCR4 and CD44 levels in BM leukemia cells from PDX mice suggesting a novel function of MCL-1, specifically the regulation of leukemia-stroma interactions. The cell intrinsic anti-apoptotic function of MCL-1 may therefore be complemented and enhanced by the cell-extrinsic enhanced adhesion to the BM stroma.

In addition to MCL-1, other mechanisms of intrinsic and acquired venetoclax resistance were reported in recent years.[47-50] Although highly effective and statistically significantly extending survival, our combination-treated mice eventually died of leukemia. We observed increased p-AKT levels in leukemia cells collected from these mice, which warrants further investigation.

Collectively, we demonstrated that MCL-1 regulates cell metabolism, leukemia-stroma interactions, and protects leukemia cells from BCL-2 inhibition. MCL-1 inhibition targets multiple cancer cell characteristics and therefore has multifaceted effects in AML. The MCL-1 inhibition-mediated suppression of metabolic activity and inhibition of CXCR4 and CD44 may contribute to its efficacy against AML stem cells in the BM stromal microenvironment. Treatment strategies involving combined MCL-1 and BCL-2 inhibition could improve the outcomes in AML patients for whom BCL-2-targeted therapy has failed, which warrants further clinical evaluation.

References

1. Konopleva M, Contractor R, Tsao T, et al. Mechanisms of apoptosis sensitivity and resistance to the BH3 mimetic ABT-737 in acute myeloid leukemia. Cancer Cell. 2006;10(5):375-388.
2. Pan R, Hogdal LJ, Benito JM, et al. Selective BCL-2 inhibition by ABT-199 causes on-target cell death in acute myeloid leukemia. Cancer Discov. 2014;4(3):362-375.
3. Schoenwaelder SM, Jarman KE, Gardiner EE, et al. Bcl-xL-inhibitory BH3 mimetics can induce a transient thrombocytopathy that undermines the hemostatic function of platelets. Blood. 2011;118(6):1663-1674.
4. Konopleva M, Pollyea DA, Potluri J, et al. Efficacy and biological correlates of response in a phase II study of venetoclax monotherapy in patients with acute myelogenous leukemia. Cancer Discov. 2016;6(10):1106-1117.
5. DiNardo CD, Pratz K, Pullarkat V, et al. Venetoclax combined with decitabine or azacitidine in treatment-naive, elderly patients with acute myeloid leukemia. Blood. 2019;133(1):7-17.
6. DiNardo CD, Pratz KW, Letai A, et al. Safety and preliminary efficacy of venetoclax with decitabine or azacitidine in elderly patients with previously untreated acute myeloid leukaemia: a non-randomised, open-label, phase 1b study. Lancet Oncol. 2018;19(2):216-228.
7. Pollyea DA, Stevens BM, Jones CL, et al. Venetoclax with azacitidine disrupts energy metabolism and targets leukemia stem cells in patients with acute myeloid leukemia. Nat Med. 2018;24(12):1859-1866.
8. De Blasio A, Vento R, Di Fiore R. Mcl-1 targeting could be an intriguing perspective to cure cancer. J Cell Physiol. 2018;233(11):8482-8498.
9. Adams JM, Cory S. The BCL-2 arbiters of apoptosis and their growing role as cancer targets. Cell Death Differ. 2018;25(1):27-36.
10. Glaser SP, Lee EF, Trounson E, et al. Anti-apoptotic Mcl-1 is essential for the development and sustained growth of acute myeloid leukemia. Genes Dev. 2012;26(2):120-125.
11. Campbell CJ, Lee JB, Levadoux-Martin M, et al. The human stem cell hierarchy is defined by a functional dependence on Mcl-1 for self-renewal capacity. Blood. 2010;116(9):1433-1442.
12. Pan R, Ruvolo VR, Wei J, et al. Inhibition of Mcl-1 with the pan-Bcl-2 family inhibitor (-)BI97D6 overcomes ABT-737 resistance in acute myeloid leukemia. Blood. 2015;126(3):363-372.
13. Yoshimoto G, Miyamoto T, Jabbarzadeh-Tabrizi S, et al. FLT3-ITD up-regulates MCL-1 to promote survival of stem cells in acute myeloid leukemia via FLT3-ITD-specific STAT5 activation. Blood. 2009;114(24):5034-5043.
14. Kaufmann SH, Karp JE, Svingen PA, et al. Elevated expression of the apoptotic regulator Mcl-1 at the time of leukemic relapse. Blood. 1998;91(3):991-1000.
15. Bose P, Gandhi V, Konopleva M. Pathways and mechanisms of venetoclax resistance. Leuk Lymphoma. 2017;58(9):1-17.
16. Niu X, Zhao J, Ma J, et al. Binding of released Bim to Mcl-1 is a mechanism of intrinsic resistance to ABT-199 which can be overcome by combination with daunorubicin or cytarabine in AML cells. Clin Cancer Res. 2016;22(17):4440-4451.
17. Huang H, Shah K, Bradbury NA, Li C, White C. Mcl-1 promotes lung cancer cell migration by directly interacting with VDAC to increase mitochondrial Ca2+ uptake and reactive oxygen species generation. Cell Death Dis. 2014;5:(10)e1482.
18. Lee KM, Giltnane JM, Balko JM, et al. MYC and MCL1 cooperatively promote chemotherapy-resistant breast cancer stem cells via regulation of mitochondrial oxidative phosphorylation. Cell Metab. 2017;26(4):633-647.
19. Farge T, Saland E, de Toni F, et al. Chemotherapy-resistant human acute myeloid leukemia cells are not enriched for leukemic stem cells but require oxidative metabolism. Cancer Discov. 2017;7(7):716-735.
20. Liyanage SU, Hurren R, Voisin V, et al. Leveraging increased cytoplasmic nucleoside kinase activity to target mtDNA and oxidative phosphorylation in AML. Blood. 2017;129(19):2657-2666.
21. Testa U, Labbaye C, Castelli G, Pelosi E. Oxidative stress and hypoxia in normal and leukemic stem cells. Exp Hematol. 2016;44(7):540-560.
22. Kotschy A, Szlavik Z, Murray J, et al. The MCL1 inhibitor S63845 is tolerable and effective in diverse cancer models. Nature. 2016;538(7626):477-482.
23. Tron AE, Belmonte MA, Adam A, et al. Discovery of Mcl-1-specific inhibitor AZD5991 and preclinical activity in multiple myeloma and acute myeloid leukemia. Nat Commun. 2018;9(1):5341.
24. Caenepeel S, Brown SP, Belmontes B, et al.

AMG 176, a selective MCL1 inhibitor, is effective in hematologic cancer models alone and in combination with established therapies. Cancer Discov. 2018;8(12):1582-1597.

25. Cidado J, Boiko S, Proia T, et al. AZD4573 is a highly selective CDK9 inhibitor that suppresses Mcl-1 and induces apoptosis in hematological cancer cells. Clin Cancer Res. 2019;26(4):922-934.

26. Teh TC, Nguyen NY, Moujalled DM, et al. Enhancing venetoclax activity in acute myeloid leukemia by co-targeting MCL1. Leukemia. 2018;32(2):303-312.

27. Pan R, Ruvolo V, Mu H, et al. Synthetic lethality of combined Bcl-2 inhibition and p53 activation in AML: mechanisms and superior antileukemic efficacy. Cancer Cell. 2017;32(6):748-760.

28. Daver NG, Garcia JS, Jonas BA, et al. Updated results from the venetoclax (Ven) in combination with idasanutlin (Idasa) arm of a phase 1b trial in elderly patients (Pts) with relapsed or refractory (R/R) AML ineligible for cytotoxic chemotherapy. Blood. 2019;134(Suppl 1):S229-229.

29. Moujalled DM, Pomilio G, Ghiurau C, et al. Combining BH3-mimetics to target both BCL-2 and MCL1 has potent activity in preclinical models of acute myeloid leukemia. Leukemia. 2019;33(4):905-917.

30. Ramsey HE, Fischer MA, Lee T, et al. A novel MCL1 inhibitor combined with venetoclax rescues venetoclax-resistant acaute myelogenous leukemia. Cancer Discov. 2018;8(12):1566-1581.

31. Konopleva M, Andreeff M. Targeting the leukemia microenvironment. Curr Drug Targets. 2007;8(6):685-701.

32. Carter BZ, Mak PY, Wang X, et al. An ARC-regulated IL1β/Cox-2/PGE2/β-Catenin/ARC circuit controls leukemia-microenvironment interactions and confers drug resistance in AML. Cancer Res. 2019;79(6):1165-1177.

33. Studeny M, Marini FC, Champlin RE, Zompetta C, Fidler IJ, Andreeff M. Bone marrow-derived mesenchymal stem cells as vehicles for interferon-beta delivery into tumors. Cancer Res. 2002;62(13):3603-3608.

34. Carter BZ, Mak PY, Mu H, et al. Combined targeting of BCL-2 and BCR-ABL tyrosine kinase eradicates chronic myeloid leukemia stem cells. Sci Transl Med. 2016;8(355):355ra117.

35. Carter BZ, Mak PY, Wang X, et al. Focal adhesion kinase as a potential target in AML and MDS. Mol Cancer Ther. 2017;16(6):1133-1144.

36. Han L, Qiu P, Zeng Z, et al. Single-cell mass cytometry reveals intracellular survival/proliferative signaling in FLT3-ITD-mutated AML stem/progenitor cells. Cytometry A. 2015;87(4):346-356.

37. Zhou H, Mak PY, Mu H, et al. Combined inhibition of beta-catenin and Bcr-Abl synergistically targets tyrosine kinase inhibitor-resistant blast crisis chronic myeloid leukemia blasts and progenitors in vitro and in vivo. Leukemia. 2017;31(10):2065-2074.

38. Chen H, Lau MC, Wong MT, Newell EW, Poidinger M, Chen J. Cytofkit: a bioconductor package for an integrated mass cytometry data analysis pipeline. PLoS Comput Biol. 2016;12(9):e1005112.

39. Chou TC, Talalay P. Quantitative analysis of dose-effect relationships: the combined effects of multiple drugs or enzyme inhibitors. Adv Enzyme Regul. 1984;22:27-55.

40. Sun Y, Bandi M, Lofton T, et al. Functional genomics reveals synthetic lethality between phosphogluconate dehydrogenase and oxidative phosphorylation. Cell Rep. 2019;26(2):469-482.

41. Gelman SJ, Naser F, Mahieu NG, et al. Consumption of NADPH for 2-HG synthesis increases pentose phosphate pathway flux and sensitizes cells to oxidative stress. Cell Rep. 2018;22(2):512-522.

42. Molina JR, Sun Y, Protopopova M, et al. An inhibitor of oxidative phosphorylation exploits cancer vulnerability. Nat Med. 2018;24(7):1036-1046.

43. Abraham M, Biyder K, Begin M, et al. Enhanced unique pattern of hematopoietic cell mobilization induced by the CXCR4 antagonist 4F-benzoyl-TN14003. Stem Cells. 2007;25(9):2158-2166.

44. Virappane P, Gale R, Hills R, et al. Mutation of the Wilms' tumor 1 gene is a poor prognostic factor associated with chemotherapy resistance in normal karyotype acute myeloid leukemia: the United Kingdom Medical Research Council Adult Leukaemia Working Party. J Clin Oncol. 2008;26(33):5429-5435.

45. Hwang AB, Lee SJ. Regulation of life span by mitochondrial respiration: the HIF-1 and ROS connection. Aging. 2011;3(3):304-310.

46. Mathieu J, Zhang Z, Zhou W, et al. HIF induces human embryonic stem cell markers in cancer cells. Cancer Res. 2011;71(13):4640-4652.

47. Blombery P, Anderson MA, Gong JN, et al. Acquisition of the recurrent Gly101Val mutation in BCL2 confers resistance to venetoclax in patients with progressive chronic lymphocytic leukemia. Cancer Discov. 2019;9(3):342-353.

48. Chen X, Glytsou C, Zhou H, et al. Targeting mitochondrial structure sensitizes acute myeloid leukemia to venetoclax treatment. Cancer Discov. 2019;9(7):890-909.

49. Nechiporuk T, Kurtz SE, Nikolova O, et al. The TP53 apoptotic network is a primary mediator of resistance to BCL2 inhibition in AML cells. Cancer Discov. 2019;9(7):910-925.

50. Zhao X, Ren Y, Lawlor M, et al. BCL2 amplicon loss and transcriptional remodeling drives ABT-199 resistance in B cell lymphoma models. Cancer Cell. 2019;35(5):752-766.